Desalination and Water Treatment
www.deswater.com

doi: 10.5004/dwt.2017.0808

60 (2017) 137–143
January

Preparation and characterization of PAN/CNT nanocomposite fiber supports for membrane filtration

Evrim Celik Madenli[a,*], Ozgur Cakmakci[b]

[a]*Department of Environmental Engineering, Suleyman Demirel University, Isparta 32260, Turkey, Tel. +90 246 211 16 91; email: evrimcelik@sdu.edu.tr*
[b]*Department of Environmental Engineering, Mus Alpaslan University, Mus 32260, Turkey, Tel. +90 436 249 49 49; email: o.cakmakci@alparslan.edu.tr*

Received 15 July 2016; Accepted 17 November 2016

ABSTRACT

Polymeric membranes have low mechanical, chemical, and thermal resistances, whereas carbon nanotubes (CNTs) have excellent mechanical properties, in addition to high chemical and thermal stability. Hence, polyacrylonitrile/multiwalled CNT (PAN/CNT) nanocomposite fibers were synthesized via an electrospinning process in order to modify the properties of PAN nanofibers. The resultant nanofibers were then characterized by scanning electron microscopy, transmission electron microscopy and Fourier transform infrared spectroscopy. It was found that the addition of CNTs into the polymer solution increased the roughness of the fiber surface. The diameters of the PAN, 0.1% CNT doped PAN and 0.5% CNT doped PAN nanofibers are 1.63, 0.59 and 1.39 μm, respectively. Hence, the thickness of the nanocomposite fiber was seen to be dependent on the CNT concentration. The protein adsorption onto the 0.1% CNT doped PAN nanofibers and 0.5% CNT doped PAN nanofibers were 26% and 34% less than the PAN nanofibers, respectively. Hence, adding CNTs to the PAN/CNT nanocomposite fibers also had the potential to alleviate fouling. Based on these results, the modification of PAN/CNT nanocomposite fibers was confirmed, and these fibers were deemed to be a good alternative to current support materials for membranes.

Keywords: Carbon nanotubes; Electrospinning; Membrane; Membrane support; Polyacrylonitrile

---

1. Introduction

Membrane phenomena were first observed in the eighteenth century. However, even though the elements of modern membrane science were developed in the 1960s, they were used only in laboratory-scale studies [1]. Membrane operations use a membrane to execute a particular separation, and due to either physical or chemical differences between the membrane and permeating components, membranes can transport some elements more readily than others [2]. To date, their cost, unreliability, low speed, and unselectivity have prohibited their widespread use as a separation process [1], though over the last decades membrane processes have been developed within specific industries [3]. Hence, this form of development ensures that neither a single type of membrane nor a single technology has been developed [4]. Indeed, membrane operations can be classified according to the driving force, mechanism of separation, structure of the membrane, and the phases in contact [5]; most membrane operations are governed by pressure, concentration, electrical potential, or temperature gradients [4].

Polymeric membranes are widely being used in membrane operations due to their good film-forming ability, flexibility, toughness, separation properties, and low cost. However, they have low mechanical, chemical, and thermal resistances, and poor anti-fouling ability because of their hydrophobic nature [6]. Furthermore, even though polyacrylonitrile (PAN) based membranes have good chemical stability and filtration performance, they are very prone to fouling [7].

---

* Corresponding author.

1944-3994/1944-3986

Nanosized organic or inorganic material blended composite membranes are attractive because of their enhanced properties, which include high permselectivity, good hydrophilicity, and improved fouling resistance [6]. For example, polymeric nanocomposites have the potential to be used in a wide range of applications due to their easy processability, low cost, and good adhesion to substrates [8]. Since their discovery in 1991 by Iijima [9], carbon nanotubes (CNTs) have attracted interest because of their excellent mechanical properties, high chemical and thermal stability, and high aspect ratio [10]. Overall, CNTs have the potential to improve the material properties of polymers due to their high aspect ratio, at a low density with high strength and stiffness [11].

Since its discovery in 1934, electrospinning has attracted continued interest due to its potential for use in fabricating different types of nanofibers [12]. Notably, nanofibers prepared by electrospinning have a small diameter, high aspect ratio, large specific surface area, composition diversity, unique physicochemical properties, and design flexibility for chemical/physical surface functionalization [8].

Polymer/CNT fibers are more suitable than bulk polymer/CNT composites for many applications. Moreover, it is possible to align the nanotubes in a polymer matrix using various fiber production techniques [13]. Examples of polymer/CNT composite fiber preparation methods include the following. Andrews et al. [14] prepared composite carbon fibers having isotropic petroleum pitch matrices and CNTs using a single-hole fiber spinning apparatus. They showed that these composite carbon fibers had enhanced mechanical and electrical properties. Naebe et al. [15] synthesized polyvinyl alcohol (PVA) nanofibers having CNTs, using an electrospinning method. They showed that the CNTs caused an apparent increase in the crystallinity of PVA. Wan et al. [16] then showed that vibration electrospinning increased the dispersion and alignment of CNTs in PAN nanofibers, compared with traditional electrospinning techniques. Khan et al. prepared graphene nanoflakes embedded PAN nanofibers by electrospinning [17]. They showed that the physical properties, such as wettability, dielectric constant, ionic conductivity, and thermal conductivity values of the PAN nanocomposites increased as a function of graphene concentrations. Khan et al. prepared CNT incorporated PAN nanofibers by electrospinning [18]. They showed that the CNT incorporation increased the thermal conductivity of the nanofibers more than tenfold.

In our previous publications, it was shown that there might be hydrogen-bonding interactions between functionalized CNTs and polyethersuflone [19]. Based on these considerations and the body of previous research, the objective of this work is to synthesize CNT-doped PAN nanocomposite fibers by electrospinning as a support material for membranes. To subsequently characterize the PAN/CNT nanofibers, Fourier transform infrared (FTIR) spectroscopy, transmission electron microscopy (TEM), and scanning electron microscopy (SEM) were employed.

2. Materials and methods

2.1. Materials

PAN (molecular weight: 150,000) and anhydrous N,N dimethylformamide (DMF; 99.8%) were purchased from Polysciences Inc. (USA) and Sigma (USA), respectively. CNTs (diameter: 20–30 nm) were supplied by Nanostructured and Amorphous Materials Inc. (USA). In addition, bovine serum albumin (BSA) having a molecular weight of 68 kDa, molecular size of 14 nm × 4 nm × 4 nm, and an isoelectric point of pH 4.7–4.9 [20] was purchased from Sigma (USA). All materials were used as-received without further treatment.

2.2. CNT modification

The chemical modification of CNTs in concentrated sulfuric and nitric acid is described elsewhere [19,21]. In brief, raw CNTs were modified in a 3:1 (v/v) HNO_3:H_2SO_4 mixture at 70°C for 9 h under ultrasonication. Modified CNTs were then washed using Deionized (DI) water and filtered until a neutral pH was attained, before being dried overnight in a vacuum oven at 100°C.

2.3. Nanocomposite fiber fabrication

CNT-doped PAN nanofibers were synthesized via electrospinning. The nanofiber solutions were prepared as follows. CNTs were ultrasonicated in DMF to ensure good dispersion. After dispersing CNTs in the solvent, PAN (13 wt%) was dissolved in the dope solution under continuous stirring and heating at 80°C until the PAN was completely dissolved and the solution became homogenous. The resultant polymer solution was then ultrasonicated to remove air bubbles; after air bubble removal, electrospinning was applied to synthesize the nanofibers.

Control and CNT-reinforced PAN nanocomposite fibers were all prepared using an automated electrospinning instrument (NE100, Inovenso Co. Ltd., Turkey), as schematically shown in Fig. 1. In the figure, an electric field was generated between a nozzle system and a grounded collection drum, which rotated constantly at 350 rpm. The nozzle system consisted of a tube having four nozzles, each having a 700-μm inner diameter. The polymer solution was pumped into the system with a syringe pump, and nanofibers were collected on a non-woven fabric. The voltage of the solution, distance between the nozzles and collection drum, and feed rate of all polymer solutions were optimized; for each polymer solution, electrospinning was applied under the values given in Table 1. Note that nanofibers marked as PAN/CNT-0.25 refer to nanofibers prepared in a solution in which the content of the CNTs with respect to PAN was 0.25% by weight.

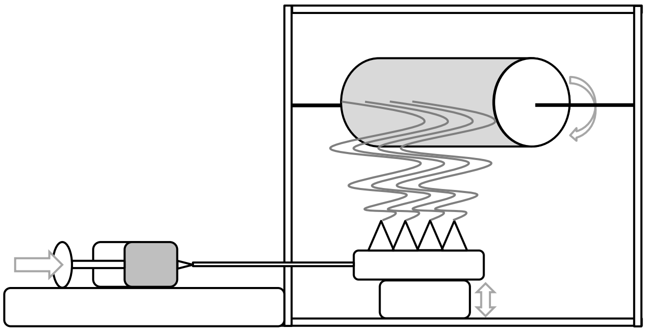

Fig. 1. Schematic representation of electrospinning setup.

Table 1
Electrospinning characteristics

Nanofiber name	CNT ratio (%)	Voltage (kV)	Feed rate (mL/h)	Distance (cm)
PAN	0	33,8	8	16
PAN/CNT-0.1	0.1	32	7.5	16
PAN/CNT-0.25	0.25	32	8	16
PAN/CNT-0.5	0.5	35	12	16

2.4. Characterization

The morphology of the raw and modified CNTs and also the orientation of the CNTs in the fibers were analyzed by TEM (G2 F20; FEI Tecnai, USA). The surface morphologies of the nanofibers were directly observed by SEM (Quanta FEG 250; FEI, USA), and the structures of the raw and modified CNTs and nanofibers were characterized by FTIR (Spectrum Two, PerkinElmer, USA). The viscosities of the polymer solutions were determined using a viscosimeter (Vibro, AND, Japan).

2.5. Protein adsorption

BSA was chosen as the protein source for evaluating the adsorptive fouling property of the membranes. In the BSA adsorption experiments, membranes were cut into small pieces and immersed into a 1-mg/mL BSA solution and gently shaken at room temperature for 4 h. The solution was maintained at pH 7 using PBS or at pH 3 using NaOH and HCl, as needed. The membrane coupons were then washed in DI water and ultrasonicated for 2 min. Thereafter, the amount of adsorbed BSA was directly measured using a UV-vis spectrometer (UV-VIS Spectrophotometer, Shimadzu, Japan) via its absorbance at 280 nm. The average of at least two measurements was reported.

3. Results and discussion

3.1. CNT modification

TEM images of the raw and modified CNTs are given in Fig. 2. In Fig. 2(A), raw CNTs were around tens of micrometers in length, and most of the tips of the CNTs were closed (Fig. 2(B)), though subsequent treatment with a strong acid mixture shortened the lengths of the CNTs to around 500 μm (Figs. 2(C) and (D)). Hence, the tips of the shortened CNTs are open due to the sonication and the treatment with the strong acid mixture.

FTIR spectra of the raw and modified CNTs are shown in Fig. 3. There are very small two peaks ~3,440 and 1,630 cm^{-1} on pure CNTs. However, modified CNTs exhibited very clear three peaks: ~3,440 cm^{-1} (–OH), ~1,630 cm^{-1} (>C=O) [22,23], and ~1,460 cm^{-1} (O-C=O) [24]. These TEM and FTIR results confirm the successful modification of the CNTs obtained by using an acid mixture. This observation also confirms that the surface of the CNTs functionalized by strong acid mixture and the terminal carbons on the CNTs were converted to carboxylic groups [25].

3.2. Electrospun nanofibers

The viscosities of the polymer solutions for nanofiber synthesis are given in Table 2, where it is seen that the viscosity of the 0.1% CNT added PAN solution is higher than the viscosity of the pure PAN solution. Overall, the viscosities of the CNT-doped PAN solutions increased when increasing the CNT concentration in the solution. This increased viscosity subsequently improved the dispersion of CNTs in

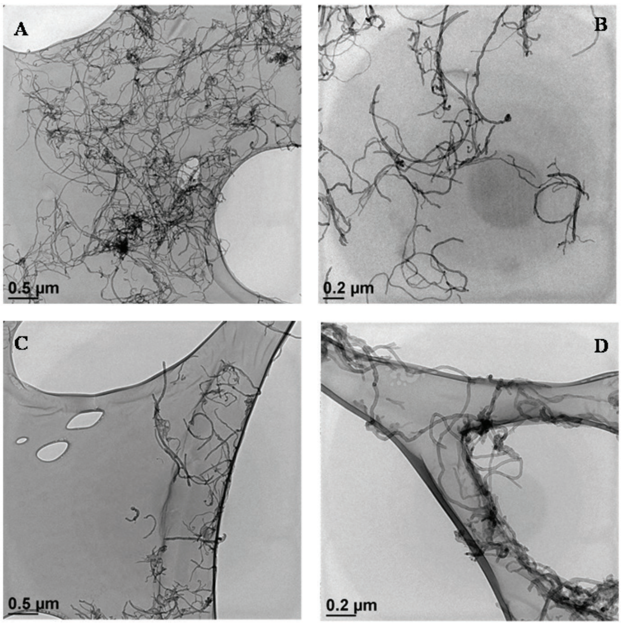

Fig. 2. TEM images of (A), (B) raw and (C), (D) modified CNTs.

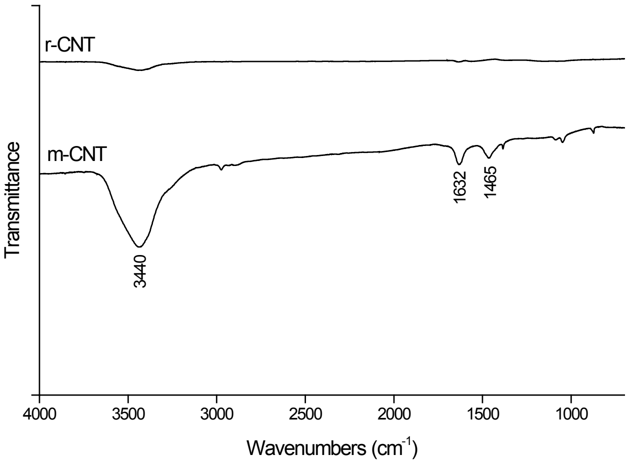

Fig. 3. FTIR spectra of the raw (r-CNT) and modified (m-CNT) CNTs.

Table 2
Viscosities of the polymer solutions

Polymer solution	Viscosity (Pa.s)
PAN	1.19
PAN/CNT-0.1	1.64
PAN/CNT-0.25	1.66
PAN/CNT-0.5	3.70

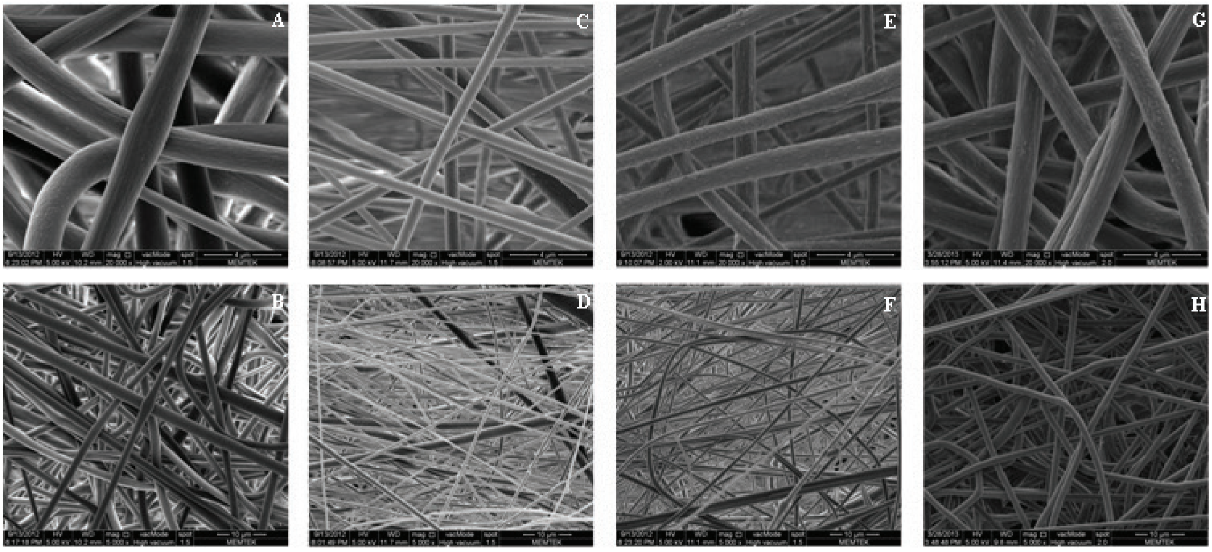

Fig. 4. SEM images of: (A), (B) PAN; (C), (D) PAN/CNT-0.1; (E), (F) PAN/CNT-0.25; and (G), (H) PAN/CNT-0.5 nanofibers. (The dimensions of the scale bars are 4 μm on (A), (C), (E) and (G), and 10 μm on (B), (D), (F) and (H).)

the polymer solution, though the huge viscosity increase observed by the introduction of CNTs might be due to the agglomeration of CNTs in the polymer solution [26].

The color of the pure PAN nanofibers was white, whereas the PAN/CNT fibers were grey. The surface morphologies of the PAN/CNT nanocomposite fibers were subsequently characterized by SEM micrographs (Fig. 4). PAN nanofibers are seen to be smooth (Fig. 4(A)), with the roughnesses of the nanofibers increasing with further increases in the CNT concentration (Figs. 4(C), (E), and (G)). Okiel et al. also confirmed the increased surface roughness of the polypropylene membranes by addition of CNTs [27]. This roughness might be due to the ends of the CNTs sticking out of the fiber surface [28]; these CNTs are thought to be the source of the good adhesion to the polymer if nanocomposite fibers are to be used as a membrane support material. Moreover, the increased roughness also provides good adhesion to the polymer surfaces.

In Fig. 4, there are no imperfections such as beads formed in any of the nanocomposite fibers (Figs. 4(B), (D), (F) and (H)). The fiber quality of the electrospinning process is thus seen to be dependent on a balance between the electrostatic repulsion, surface tension, and viscoelastic forces. When the viscosity of the solution increases, the surface tension was suppressed by electrostatic repulsion and viscoelastic forces. Formations of the fibers are favored by the dominating viscoelastic forces [8], resulting in the formation of fibers having bead-free and smooth surfaces (Fig. 4).

Variations of the fiber diameters were determined using AxioVision Rel. 4.8 to view 20 nanofibers from 20 different images for each fiber. The average nanofiber diameters are shown in Fig. 5, with the diameters of the CNT-doped nanofibers being smaller than the diameters of the PAN nanofibers. Moreover, the diameters of the nanofibers increased with an increase in the CNT concentration. Based on a one-way ANOVA test, there is a significant difference between the diameters of the nanofibers synthesized. These results can also be visualized in the SEM images (Figs. 4(A), (C), (E) and (G)). The gradual decrease of the diameters of the PAN/CNT nanofibers compared with PAN nanofibers might be due to the increased conductivities of the CNT-doped nanofibers due to the conductive CNTs. In addition, the increase in the fiber diameters of the nanofibers observed when increasing the CNT concentration might be due to the increased viscosities that occurred when the CNT concentration was increased (Table 2) [28].

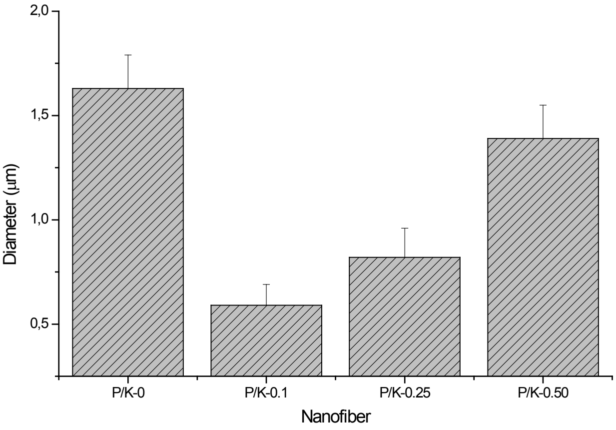

Fig. 5. Diameters of the nanofibers.

Fig. 6 presents the FTIR spectra of the surfaces of the PAN and PAN/CNT nanofibers having 0%–0.5% CNTs. The peaks at ~2,950 cm^{-1}, ~2,850 cm^{-1}, and ~1,050 cm^{-1} observed in both the PAN and PAN/CNT nanofibers indicate C-H of $-CH_2$ in acrylonitrile, C-H of $-CH_2$ in acid, and $C-CH_3$ or $C-CH_2-COOH$, respectively [29]. The PAN/CNT nanofibers are noticeably different from the bare PAN nanofibers, with two new peaks at ~1,670 and ~1,455 cm^{-1}, related to the >C=O and O-C=O groups on CNTs loaded in nanofibers, respectively.

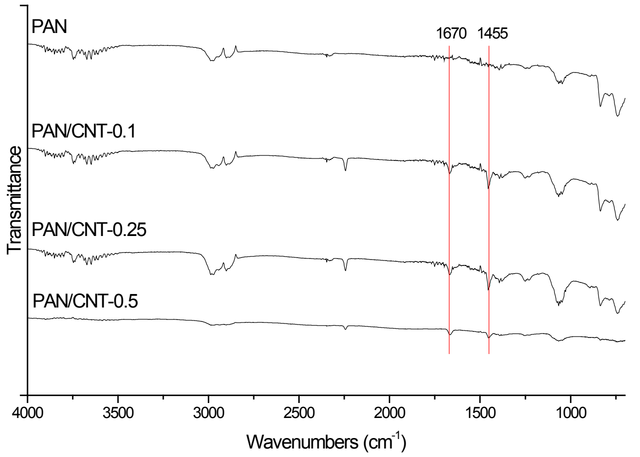

Fig. 6. FTIR spectra of PAN, PAN/CNT-0.1, PAN/CNT-0.25, and PAN/CNT-0.5.

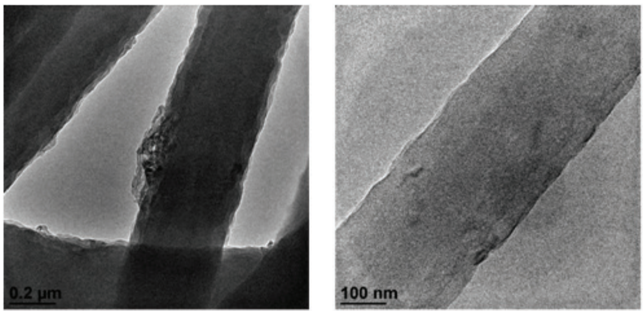

Fig. 7. TEM images of PAN/CNT-0.5 nanofiber.

This result clearly confirms the successful incorporation of CNTs into the PAN composite nanofibers.

Fig. 7 shows the TEM images of PAN/CNT-0.5 nanofibers. In the figure, CNTs were aligned along the axes of the PAN nanofibers, which is consistent with the results of Lisunova et al. [30]. There are three possible mechanisms for aligning CNTs in the nanofibers: flow-induced confinement, high-charge induced alignment, and fiber diameter confinement induced orientation during electrospinning [31].

3.3. Protein adsorption

BSA adsorption onto PAN and PAN/CNT nanocomposite fibers are demonstrated in Fig. 8. The isoelectric point of BSA is around 4.7 [20,32]. Carboxyl functionalized CNTs increases the negative zeta potential of PAN membranes [33]. At pH 3, electrostatic attraction occurs since the protein and all fibers had opposite charges. Moreover, at pH values below the isoelectric point, protein denaturation is relatively high [34,35]; hence, the highest protein adsorptions were seen at pH 3. At pH 7, both the BSA and nanocomposite fiber surfaces were negatively charged, such that electrostatic repulsion was dominant between the fiber surfaces and the protein. Overall, protein adsorption decreased with increases in the CNT concentration in the dope solution, at both pH 3 and 7, thus indicating the potential of using CNTs to alleviate fouling.

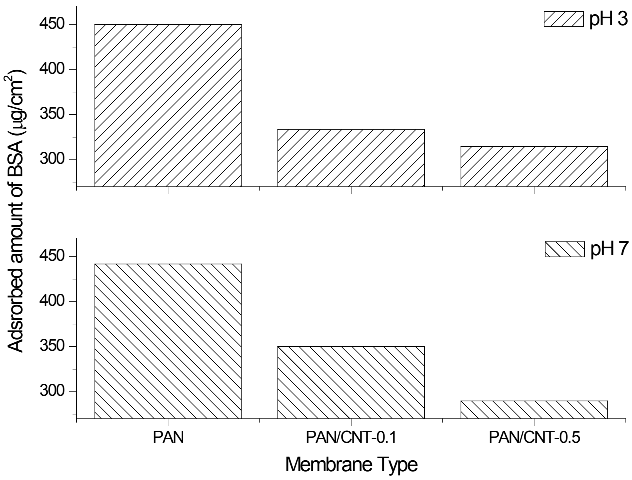

Fig. 8. BSA adsorption on PAN/CNT nanofiber mats at pH 3 and 7 (average BSA adsorption of two replicates are reported).

Filtration membranes are the most common media for separation tasks. However, they need a support layer because of their fragile nature in order to remain robust under practical operating conditions. Guechi et al. prepared anorthite and Harabi et al. prepared aluminosilicate tubular ceramic supports for microfiltration and ultrafiltration membranes [36,37]. Polymeric membranes are widely used in filtration operations, and there is a necessity of a polymeric supports for polymeric membranes to improve their lifespan and material properties. Dumee et al. showed the improved membrane distillation performances of the composite CNT membranes compared with the pure self-supporting CNT membranes [38]. The CNT-doped PAN nanocomposite fibers developed here are a potential alternative to serve as a support material for filtration membranes. Guclu et al. prepared PAN/PSU fibers and proposed to be used as disposable membranes such as are used in syringe filters [39]. Similarly, these CNT-doped PAN nanocomposite fiber mats can be used as disposable membranes such as in syringe filters with their improved material properties.

4. Conclusions

PAN/CNT nanocomposite fibers were successfully prepared via electrospinning. Prior to fiber synthesis, CNTs were functionalized using a strong acid mixture to increase their dispersion in an organic solvent. The tips of the shortened CNTs are open due to the sonication and the treatment with the strong acid mixture. Moreover, the terminal carbons on the CNTs were converted to carboxylic groups.

Even though the PAN nanofibers are smooth, the roughnesses of the nanofibers increase by increasing CNT concentration. The diameters of the PAN, PAN/CNT-0.1, PAN/CNT-0.25 and PAN/CNT-0.5 nanofibers are 1.63, 0.59, 0.82 and 1.39 μm, respectively. That is, the diameters of the nanofibers decreased by CNT addition but the diameters of the nanofibers increased with an increase in the CNT concentration. Therefore, the roughness and thickness of the nanocomposite fibers were found to depend on the concentration of CNTs in the nanocomposite.

Protein adsorptions onto PAN/CNT-0.1 and PAN/CNT-0.5 nanofibers are 26% and 34% lower than the PAN nanofibers. Hence, protein adsorption of the nanocomposite fibers was alleviated by the addition of CNTs into the fiber structure. These PAN/CNT nanocomposite fiber mats can be used as disposable membranes such as in syringe filters with their reduced fouling tendency. In addition, PAN/CNT nanocomposite fibers are deemed to be a good alternative to current support materials for membranes.

Acknowledgments

The authors gratefully acknowledge the National Research Center on Membrane Technologies (MEM-TEK), Istanbul Technical University for their contribution of electrospinning instrument usage. This research was supported by a grant (111R012) from the Scientific and Technological Research Council of Turkey, through the Support Program for Scientific and Technological Research Projects, and in part supported by a grant (SDU-3785) from Suleyman Demirel University through the Scientific Research Projects Programme.

References

[1] R.W. Baker, Membrane Technology and Applications, 2nd ed. John Wiley & Sons, England, 2004.
[2] M. Mulder, Basic Principles of Membrane Technology, Kluwer Academic Publishers, The Netherlands, 1997.
[3] J.F. Blanco, Q.T. Nguyen, P. Schaetzel, Novel hydrophilic membrane materials: sulfonated polyethersulfone Cardo, J. Membr. Sci., 186 (2001) 267–279.
[4] P.T. Cardew, M.S. Le, Membrane Processes: A Technology Guide, The Royal Society of Chemistry, UK, 1998.
[5] P. Aptel, C.A. Buckley, Categories of Membrane Operations, J. Malleviale, P.E. Odendaal, M.R. Wiesner, Eds., Water Treatment Membrane Processes, McGraw-Hill, USA, 1996.
[6] Y.N. Yang, H.X. Zhang, P. Wang, Q.Z. Zheng, J. Li, The influence of nano-sized TiO_2 fillers on the morphologies and properties of PSFUF membrane, J. Membr. Sci., 288 (2007) 231–238.
[7] T. Barroso, M. Temtem, T. Casimiro, A. Aguiar-Ricardo, Antifouling performance of poly(acrylonitrile)-based membranes: from green synthesis to application, J. Supercrit. Fluids, 56 (2011) 312–321.
[8] D. Zhang, A.B. Karki, D. Rutman, D.P. Young, A. Wang, D. Cocke, T.H. Ho, Z. Guo, Electrospun polyacrylonitrile nanocomposite fibers reinforced with Fe_3O_4 nanoparticles: fabrication and property analysis, Polymer, 50 (2009) 4189–4198.
[9] S. Iijima, Helical microtubules of graphitic carbon, Nature, 354 (1991) 56–58.
[10] Y.H. Li, S.G. Wang, J.Q. Wei, X.F. Zhang, C.L. Xu, Z.K. Luan, D. Wu, B.Q. Wei, Lead adsorption on carbon nanotubes, Chem. Phys. Lett., 357 (2002) 263–266.
[11] F.H. Gojny, M.H.G. Wichmann, U. Kopke, B. Fiedler, K. Schulte, Carbon nanotube-reinforced epoxy-compo sites: enhanced stiffness and fracture toughness at low nanotube content, Compos. Sci. Technol., 64 (2004) 2363–2371.
[12] A. Formhals, Process and Apparatus for Preparing Artificial Threads, US Patent 1,975,504; 1934.
[13] Z. Spitalsky, D. Tasis, K. Papagelis, C. Galiotis, Carbon nanotube-polymer composites: chemistry, processing, mechanical and electrical properties, Prog. Polym. Sci., 35 (2010) 357–401.
[14] R. Andrews, D. Jacques, A.M. Rao, T. Rantell, F. Derbyshire, Y. Chen, J. Chen, R.C. Haddon, Nanotube composite carbon fibers, Appl. Phys. Lett., 75 (1999) 1329–1331.
[15] M. Naebe, T. Lin, M.P. Staiger, L.M. Dai, X.G. Wang, Electrospun single-walled carbon nanotube/polyvinyl alcohol composite nanofibers: structure-property relationships, Nanotechnology, 19 (2008) 305702 (8pp).
[16] Y.Q. Wan, J.H. He, J.Y. Yu, Carbon nanotube-reinforced polyacrylonitrile nanofibers by vibration-electrospinning, Polym. Int., 56 (2007) 1367–1370.
[17] W.S. Khan, R. Asmatulu, V. Rodriguez, M. Ceylan, Enhancing thermal and ionic conductivities of electrospun PAN and PMMA nanofibers by graphene nanoflake additions for battery-separator applications, Int. J. Energy Res., 38 (2014) 2044–2051.
[18] W.S. Khan, R. Asmatulu, I. Ahmed, T.S. Ravigururajan, Thermal conductivities of electrospun PAN and PVP nanocomposite fibers incorporated with MWCNTs and NiZn ferrite nanoparticles, Int. J. Therm. Sci., 71 (2013) 74–79.
[19] E. Celik, H. Park, H. Choi, H. Choi, Carbon nanotube blended polyethersulfone membranes for fouling control in water treatment, Water Res., 45 (2011) 274–282.
[20] K. Nakamura, K. Matsumoto, Properties of protein adsorption onto pore surface during microfiltration: effects of solution environment and membrane hydrophobicity, J. Membr. Sci., 280 (2006) 363–374.
[21] J. Liu, A.G. Rinzler, H.J. Dai, J.H. Hafner, R.K. Bradley, P.J. Boul, A. Lu, T. Iverson, K. Shemilov, C.B. Huffman, F. Rodriguez-Macias, Y.S. Shon, T.R. Lee, D.T. Colbert, R.E. Smalley, Fullerene pipes, Science, 280 (1998) 1253–1256.
[22] U.J. Kim, C.A. Furtado, X.M. Liu, G.G. Chen, P.C. Eklund, Raman and IR spectroscopy of chemically processed single-walled carbon nanotubes, J. Am. Chem. Soc., 127 (2005) 15437–15445.
[23] A. Kaniyoor, R.I. Jafri, T. Arockiadoss, S. Ramaprabhu, Nanostructured Pt decorated graphene and multi walled carbon nanotube based room temperature hydrogen gas sensor, Nanoscale, 1 (2009) 382–386.
[24] N.T. Sandeep, S. Sauraj, S.M. Rajender, C. Veena, Effect of multiwalledcarbon nanotubes on the properties of poly (methylmethacrylate) in PMMA/CNT nanocomposites, Macromol.Symp., 341 (2014) 75–89.
[25] H.G. Choi, S.H. Yoon, M. Son, E. Celik, H. Park, H. Choi, Efficacy of synthesis conditions on functionalized carbon nanotube blended cellulose acetate membrane for desalination, Desal. Wat. Treat., 57 (2016) 7545–7554.
[26] A. Allaoui, N. El Bounia, Rheological and electrical transitions in carbon nanotube/epoxy suspensions, Curr. Nanosci., 6 (2010) 158–162.
[27] K. Okiel, A.H.M. El-Aassar, T. Temraz, S. El-Etriby, H.A. Shawky, Performance assessment of synthesized CNT/polypropylene composite membrane distillation for oil field produced water desalination, Desal. Wat. Treat., 57 (2016) 10995–11007.
[28] P. Heikkila, A. Harlin, Electrospinning of polyacrylonitrile (PAN) solution: effect of conductive additive and filler on the process, Express Polym. Lett., 3 (2009) 437–445.
[29] J. Liang, Single Wall Carbon Nanotube/Polyacrylonitrile Composite Fiber, Polymer, Textile and Fiber Engineering, Master of Science, Georgia Institute of Technology, Atlanta, 2004, p. 69.
[30] M. Lisunova, A. Hildmann, B. Hatting, V. Datsyuk, S. Reich, Nanofibres of CA/PAN with high amount of carbon nanotubes by core-shell electrospinning, Compos. Sci. Technol., 70 (2010) 1584–1588.
[31] H. Lam, N. Titchenal, H. Ye, Y. Gogotsi, F. Ko, Structure and Properties of Aligned Carbon Nanotubes Reinforced Nanocomposite Fibrils, J.R. Erian Armanios, Ed., Proc. Joint American Society for Composites/American Society for Testing and Materials Committee D30 – Nineteenth Technical Conference, Atlanta, 2004.
[32] S. Boributh, A. Chanachai, R. Jiraratananon, Modification of PVDF membrane by chitosan solution for reducing protein fouling, J. Membr. Sci., 342 (2009) 97–104.
[33] G. Kaminska, J. Bohdziewicz, L. Palacio, A. Hernandez, P. Pradanos, Polyacrylonitrile membranes modified with carbon nanotubes: characterization and micropollutants removal analysis, Desal. Wat. Treat., 57 (2016) 1344–1353.
[34] I.H. Huisman, P. Pradanos, A. Hernandez, The effect of protein-protein and protein-membrane interactions on membrane fouling in ultrafiltration, J. Membr. Sci., 179 (2000) 79–90.

[35] F. Pincet, E. Perez, G. Belfort, Do denatured proteins behave like polymers? Macromolecules, 27 (1994) 3424–3425.

[36] A. Guechi, A. Harabi, S. Condoum, F. Zenikheri, B. Boudaira, F. Bouzerara, L. Foughali, Elaboration and characterization of tubular supports for membranes filtration, Desal. Wat. Treat., 57 (2016) 5246–5252.

[37] A. Harabi, F. Bouzerara, S. Condom, Preparation and characterization of tubular membrane supports using centrifugal casting, Desal. Wat. Treat., 6 (2009) 222–226.

[38] L. Dumee, K. Sears, J. Schutz, N. Finn, M. Duke, S. Gray, Carbon nanotube based composite membranes for water desalination by membrane distillation, Desal. Wat. Treat., 17 (2010) 72–79.

[39] S. Guclu, M.E. Pasaoglu, I. Koyuncu, Membrane manufacturing via simultaneous electrospinning of PAN and PSU solutions, Desal. Wat. Treat., 57 (2016) 8152–8160.